

Persistent current of a two-electron quantum disk

Oleg Olendski and Chang Sub Kim

Department of Physics, Chonnam National University, Kwangju 500-757, Republic of Korea

Ok Hee Chung

Department of Physics, Suncheon National University, Suncheon 540-742, Republic of Korea

Chom Sik Lee

Department of Electronics Engineering, Honam University, Kwangju 506-090, Republic of Korea

(Received 8 October 1996)

The persistent current of a clean two-electron quantum disk subjected to perpendicular magnetic fields is studied theoretically with an emphasis on the role of the electron-electron interaction. It is shown that the interaction reduces the magnitude of currents in general and also gives rise to the discontinuities in currents at low temperatures, compared with the results from the ideal quantum disk. The latter anomalous quantum behavior appears at the particular magnetic fields, at which the crossings take places in the energy spectra, and disappears as temperature increases. We found that an exact treatment of the exchange symmetry and the spin splittings in the energy is important in specifying the precise values of the magnetic field (and the steepness of the confinement potential) to induce such quantum effects. [S0163-1829(97)03415-2]

I. INTRODUCTION

Semiconductor quantum structures where carrier motion is confined in all three spatial dimensions are usually referred to as quantum dots and have drawn intensive attention from researchers in recent years.¹⁻¹⁴ Growing theoretical interest on transport, optical, and thermodynamic properties of these synthetic ultrasmall devices is based on impressive achievements of nanotechnologies. The number of electrons in such artificial systems is changed in a controllable way and may vary from zero to a few tens or hundreds.¹⁵ Therefore, the effects of the electron-electron interaction in such small dimensions cannot be neglected for a realistic determination of physical properties. The theoretical analyses of the parabolic quantum dots revealed a rich structure of the energy spectrum, which is strongly modified due to the electron-electron scatterings.^{1,3-8} In particular, as a result of the inclusion of the Coulomb term in the Hamiltonian the ground state undergoes the spin-singlet and spin-triplet transition as a function of the magnetic field, which in turn induces the interesting oscillations in thermodynamic quantities such as heat capacity^{1,6} and magnetization.^{4,5} Recently, evidence of the electron-electron interaction in the quantum dots has been unambiguously discovered using single-electron capacitance spectroscopy.¹⁵

In this paper we consider a two-electron system, confined by a two-dimensional harmonic potential, under vertical magnetic fields. The objective is to investigate theoretically the effect of the Coulomb interaction and exchange symmetry on persistent current induced in the quantum dot, which is an important equilibrium physical property. The motivation was partially augmented by the fact that the calculated persistent current is not trivially related to the magnetization of the system considered. The experiment¹⁵ and the self-consistent calculation¹⁶ show that our adoption of the parabolic confinement for the dot potential is a very good ap-

proximation for the GaAs quantum structures. The two-particle energy eigenstates are obtained by exactly diagonalizing numerically the Hamiltonian, and then the equilibrium currents are evaluated by taking the average over the canonical ensemble. The exchange effect and anomalous Zeeman splitting are taken into account explicitly in the formulation.

We show that the transition between the spin-singlet and -triplet states is responsible for the jumps of the persistent currents that are absent in the model without interaction. However, there is always a range of magnetic-field strengths where the resulting persistent current is not affected by the interaction. It is found that the precise values of the magnetic fields that induce such interesting quantum behaviors of the current are determined by a proper treatment of the spin effects.

In a broader context, this problem is intimately related to the lively discussion on the effect of the electron-electron interaction on persistent current in mesoscopic rings, which attracted a great deal of theoretical attention after the discovery of unexpectedly high values of the currents measured in the experiments.^{17,18} The recent theoretical analyses show that the electron-electron interaction does not alter the value of the persistent current in the mesoscopic rings.¹⁹⁻²¹ As we shall illustrate below, the same is true for the quantum dots when the applied field is weak. For stronger magnetic fields, the magnitude of the persistent current is, in general, smaller compared to that of an ideal quantum dot due to scatterings.

The paper is organized as follows. In Sec. II a brief summary of the noninteracting model is presented. Then the main results for the interacting two-electron problem are provided in Sec. III. Finally, conclusions are given in Sec. IV.

II. IDEAL QUANTUM DISK

Before treating interacting electrons, we find it useful to summarize the results of the energy spectrum and associated

quantum current within the noninteracting picture. The energy levels of a spinless electron confined in the two-dimensional parabolic potential $V(\rho) = \frac{1}{2}m_e^* \omega_0^2 \rho^2$, subjected to the uniform magnetic field $\vec{B} = (0, 0, B)$ applied perpendicularly to the lateral structure, have been known for a long time.²²⁻²⁴ The result is given by

$$E_{nl}^{(0)} = \hbar \omega (2n + |l| + 1) + \frac{1}{2} l \hbar \omega_B + \frac{\hbar^2 k_z^2}{2m_e^*}, \quad (1)$$

where m_e^* is the effective mass of the electron, $\omega_B = eB/m_e^*$ is the cyclotron frequency (throughout the presentation we shall set $c \equiv 1$), and e is the absolute value of the charge of an electron. Also, n is the radial quantum number, l is the magnetic index, and k_z is the quantum number associated with the degree of freedom along the magnetic field. We define

$$\omega \equiv \left(\omega_0^2 + \frac{1}{4} \omega_B^2 \right)^{1/2}.$$

Hereafter we shall drop the degree of freedom along the magnetic field by assuming that motion in the z direction is more strongly quantized than the one in the x - y plane, as usual.^{3,14} Accordingly, we consider the quantum disk as a quasi-two-dimensional system.

In the present work we adopt the symmetric gauge for the vector potential \vec{A} ; accordingly, the azimuthal component of \vec{A} is specified to be $A_\phi = B\rho/2$. Then the energy eigenfunction of the electron in two-dimension takes the form

$$\Psi(\vec{r}) \equiv \Psi(\rho, \phi) = \frac{1}{\sqrt{2\pi}} \exp(il\phi) R_{nl}^{(0)}(\rho), \quad (2)$$

where the normalized radial wave function is given by

$$R_{nl}^{(0)}(\rho) = \frac{1}{r_{\text{eff}}} \left[\frac{n!}{(n+|l|)!} \right]^{1/2} \exp\left(-\frac{1}{4} \frac{\rho^2}{r_{\text{eff}}^2}\right) \times \left(\frac{1}{2} \frac{\rho^2}{r_{\text{eff}}^2}\right)^{|l|/2} L_n^{|l|}\left(\frac{1}{2} \frac{\rho^2}{r_{\text{eff}}^2}\right), \quad (3)$$

where $r_{\text{eff}} \equiv (\hbar/2m_e^* \omega)^{1/2}$ and $L_n^l(x)$ is the generalized Laguerre polynomial.²⁵ Here we remark that l represents the angular momentum quantum number associated with the circular motion.

Semiclassically, the circular motion of an electron implies that there is an azimuthal current. The corresponding quantum-mechanical current J_{nl} carried by the definite orbital with quantum numbers n and l can be obtained by utilizing¹³

$$J_{nl} = -\frac{1}{2\pi} \frac{e\hbar}{m_e^*} \int_0^\infty \left[\frac{l}{\rho} + \frac{e}{\hbar} A_\phi(\rho) \right] [R_{nl}^{(0)}(\rho)]^2 d\rho \quad (4)$$

$$= -\frac{e}{h} \frac{\partial E_{nl}^{(0)}}{\partial l}. \quad (5)$$

It follows directly from Eqs. (1) and (5) that

$$J_{nl} = -\frac{e}{2\pi} \times \begin{cases} -\omega + \frac{1}{2} \omega_B, & l < 0 \\ \frac{1}{2} \omega_B, & l = 0 \\ \omega + \frac{1}{2} \omega_B, & l > 0, \end{cases} \quad (6)$$

except for the result for $l=0$, since formula (5) is ill defined in this case, and thus the direct integration Eq. (4) was used. Interestingly, the outcome of Eq. (4) for $l=0$ is equivalent to the algebraic average of the right and left derivatives using Eq. (5), as noted in Ref. 9.

Then the following relations between energies and currents of the levels with the opposite signs of the magnetic index l can be obtained:

$$E_{nl}^{(0)} - E_{n,-l}^{(0)} = l \hbar \omega_B, \quad (7)$$

$$J_{nl} + J_{n,-l} = -\frac{e\omega_B}{2\pi}, \quad (8)$$

which are especially convenient for practical purposes. One can prove that Eqs. (7) and (8) are valid for any quantum structure with a cylindrically symmetric electrostatic potential subjected to the uniform magnetic field, using the differential equation for the radial wave function.

Inclusion of the coupling of the electron spin to magnetic fields, taking the spin-orbit interaction into account, leads to the additional term in Eq. (1) for the energy spectrum:

$$\Delta E^{\text{spin}} = \pm \frac{1}{4} \hbar \omega_B g^* \frac{m_e^*}{m_e}, \quad (9)$$

with g^* being the effective Landé factor and m_e the mass of a bare electron. An additional term due to spin appears also in Eq. (4) for the current density:²⁶

$$j_{nl}^{\text{spin}} = \pm \frac{1}{8\pi} \frac{e\hbar}{m_e} g^* \frac{d}{d\rho} R_{nl}^2(\rho). \quad (10)$$

After carrying out an integration over the variable ρ , one can obtain an expression for the spin contribution to the current carried by the orbital with definite quantum numbers n and l as

$$J_{nl}^{\text{spin}} = \mp \frac{e}{4\pi} \omega g^* \frac{m_e^*}{m_e} \delta_{l0}, \quad (11)$$

where $\delta_{ll'}$ is the Kronecker delta function. Equation (11) shows that the spin contribution to the current vanishes identically for all states but $l=0$. For GaAs with $g^* = -0.44$ and $m_e^* = 0.067m_e$ spin corrections in Eqs. (9) and (11) to the final results of Eqs. (1) and (6) are small. However, these terms may be of great importance in the other semiconductors such as InSb with a large negative value of g^* .

The equilibrium current I at finite temperature T in a single-electron quantum dot can be obtained by taking the thermal average of J_{nl} over the canonical ensemble. After simple algebra, we obtain

$$I = \frac{e\omega}{2\pi} \left\{ \frac{\sinh(\frac{1}{2}\beta\hbar\omega_B)}{\sinh(\beta\hbar\omega)} - \frac{1}{2} \frac{\omega_B}{\omega} \right\}, \quad (12)$$

where $\beta = 1/k_B T$. It is easy to check that the current I becomes zero in two limiting cases: (i) $\omega_B = 0$ and (ii) $\omega_0 = 0$. On the other hand, the limit of $T \rightarrow 0$ reduces Eq. (12) to Eq. (6) with $l = 0$, as expected. For a noninteracting two-electron dot the net current is simply twice the value given in Eq. (12) when the exchange effect is neglected.

The corresponding magnetization to the definite orbital with n and l is obtained to be²³

$$M_{nl} = -\mu_B \frac{m_e}{m_e^*} \left\{ \frac{1}{2} \frac{\omega_B}{\omega} (2n + |l| + 1) + l \right\}, \quad (13)$$

where $\mu_B = e\hbar/2m_e$ is the Bohr magneton. The thermal average of this can be made and the result is

$$M = -\frac{1}{2} \mu_B \frac{m_e}{m_e^*} \left[\left(1 + \frac{1}{2} \frac{\omega_B}{\omega} \right) \coth \left\{ \frac{1}{2} \beta \hbar \left(\omega + \frac{1}{2} \omega_B \right) \right\} - \left(1 - \frac{1}{2} \frac{\omega_B}{\omega} \right) \coth \left\{ \frac{1}{2} \beta \hbar \left(\omega - \frac{1}{2} \omega_B \right) \right\} \right]. \quad (14)$$

When the limit of $\omega_0 \rightarrow 0$ is taken, Eq. (14) reduces to the orbital magnetization of an electron in a uniform magnetic field.

Importantly, a comparison of Eqs. (12) and (14) indicates that the current and magnetization are not simply related to each other, as previously noted in Ref. 9. This makes the present investigation of the persistent current of interacting electrons of interest since it does not overlap with the previous calculations for the magnetization by others.⁴⁻⁶

III. TWO-ELECTRON QUANTUM DISK

In this section we turn to the Coulomb interaction between two electrons in the quantum disk. Under the coordinate transformation of the symmetric form

$$\vec{r}_{\text{c.m.}} = \frac{1}{\sqrt{2}} (\vec{r}_1 + \vec{r}_2), \quad \vec{r}_{\text{rel}} = \frac{1}{\sqrt{2}} (\vec{r}_1 - \vec{r}_2), \quad (15)$$

the interacting two-electron Hamiltonian decouples into two independent degrees of freedom, essentially the center of mass and the relative coordinates, as

$$H_{\text{c.m.}} = \frac{1}{2m_e^*} (\vec{p}_{\text{c.m.}} + e\vec{A}_{\text{c.m.}})^2 + \frac{1}{2} m_e^* \omega_0^2 r_{\text{c.m.}}^2, \quad (16)$$

$$H_{\text{rel}} = \frac{1}{2m_e^*} (\vec{p}_{\text{rel}} + e\vec{A}_{\text{rel}})^2 + \frac{1}{2} m_e^* \omega_0^2 r_{\text{rel}}^2 + \frac{1}{4\pi\epsilon} \frac{e^2}{\sqrt{2}r_{\text{rel}}}, \quad (17)$$

where $\vec{A}_{\text{c.m.}} = \frac{1}{2}\vec{B} \times \vec{r}_{\text{c.m.}}$, $\vec{A}_{\text{rel}} = \frac{1}{2}\vec{B} \times \vec{r}_{\text{rel}}$, and ϵ is the electric permittivity of the semiconductor. One should note that the relevant mass and charge to both degrees of freedom are m_e^* and $-e$, respectively. In addition, there is the spin interaction term with the magnetic field,

$$H_{\text{spin}} = g^* \mu_B \vec{S} \cdot \vec{B}, \quad (18)$$

where $\vec{S} = \vec{S}_1 + \vec{S}_2$ is the total spin and $\vec{B} = B\hat{z}$. The wave function of the system is the product of the wave functions for each degree of freedom

$$\Psi(1,2) = \Phi(\vec{r}_{\text{c.m.}}) R(\vec{r}_{\text{rel}}) \otimes \chi(1,2),$$

where χ represents the spinor. Accordingly, the total persistent current is the sum of contributions from the center-of-mass motion $J^{\text{c.m.}}$ and the contribution from the relative motion J^{rel} :

$$J = J^{\text{c.m.}} + J^{\text{rel}} + J^{\text{spin}} \approx J^{\text{c.m.}} + J^{\text{rel}}. \quad (19)$$

For the center-of-mass motion, the problem is identical to the results already presented in Sec. II. Thus one only has to consider the radial Schrödinger equation for the relative motion

$$\begin{aligned} & \frac{d^2 R(\rho)}{d\rho^2} + \frac{1}{\rho} \frac{dR(\rho)}{d\rho} + \frac{2m_e^*}{\hbar^2} \\ & \times \left(E^{\text{rel}} - \frac{1}{2} m_e^* \omega^2 \rho^2 - \frac{1}{2} \hbar \omega_B l \right. \\ & \left. - \frac{1}{4\pi\epsilon} \frac{e^2}{\sqrt{2}\rho} - \frac{\hbar^2 l^2}{2m_e^* \rho^2} \right) R(\rho) = 0. \quad (20) \end{aligned}$$

Since the analytical solution to Eq. (20) is not known, typically one utilizes miscellaneous methods for its solution.^{3-8,10,27,28} In the present work, we expand the solution in the basis of the eigenstates of the single-electron relative Hamiltonian as

$$R_{nl}(\rho) = \sum_{n'=0}^{\infty} C_{nn'} R_{n'l}^{(0)}(\rho), \quad (21)$$

where $R_{n'l}^{(0)}(\rho)$ are given in Eq. (3) and the coefficients $C_{nn'}$ obey the normalization condition $\sum_{n'=0}^{\infty} |C_{nn'}|^2 = 1$. Then the energy eigenvalues of the relative motion are obtained from the requirement of making the determinant of the infinite system of linear homogeneous algebraic equations vanish:

$$\det |(E_{n'l}^{(0)} - E^{\text{rel}}) \delta_{n'n''} + \Delta_{n'n''}| = 0, \quad n', n'' = 0, 1, 2, \dots \quad (22)$$

The terms $\Delta_{n'n''}$ appearing in Eq. (22), which are due to the electron-electron scattering, are given as

$$\begin{aligned} \Delta_{n'n''} &= \frac{1}{2} \frac{e^2}{4\pi\epsilon} \frac{1}{r_{\text{eff}}} \left(\frac{n'!}{(n' + |l|)!} \frac{n''!}{(n'' + |l|)!} \right)^{1/2} \\ & \times \int_0^{\infty} e^{-x} x^{|l|-1/2} L_n^{|l|}(x) L_{n''}^{|l|}(x) dx. \quad (23) \end{aligned}$$

The current carried by the relative motion is obtained in the usual manner with the use of Eq. (4) from

$$\begin{aligned}
J_{nl}^{\text{rel}} = & -\frac{e\omega_0}{2\pi} \left\{ \left(1 + \frac{1}{4} \frac{\omega_B^2}{\omega_0^2} \right)^{1/2} l \right. \\
& \times \sum_{n', n''=0}^{\infty} \left[\left(\frac{n'!}{(n'+|l|)!} \frac{n''!}{(n''+|l|)!} \right)^{1/2} \right. \\
& \left. \left. \times C_{nn'} C_{nn''} \int_0^{\infty} e^{-x} x^{|l|-1} L_{n'}^{|l|}(x) L_{n''}^{|l|}(x) dx \right] + \frac{1}{2} \frac{\omega_B}{\omega_0} \right\}. \quad (24)
\end{aligned}$$

From a numerical point of view it turns out to be convenient that the integrals in Eqs. (23) and (24) can be evaluated analytically as²⁹

$$\begin{aligned}
& \int_0^{\infty} e^{-x} x^{|l|-1/2} L_{n'}^{|l|}(x) L_{n''}^{|l|}(x) dx \\
& = \frac{(|l|+n_{\min})! \Gamma(n_{\max}+1/2) \Gamma(|l|+1/2)}{\pi^{1/2} (|l|)! n_{\min}! n_{\max}!} \\
& \times {}_3F_2 \left(-n_{\min}, |l| + \frac{1}{2}, \frac{1}{2}; |l| + 1, \frac{1}{2} - n_{\max}; 1 \right) \quad (25)
\end{aligned}$$

and

$$\int_0^{\infty} e^{-x} x^{|l|-1} L_{n'}^{|l|}(x) L_{n''}^{|l|}(x) dx = \frac{(|l|+n_{\min})!}{n_{\min}! |l|!}. \quad (26)$$

In Eqs. (25) and (26) ${}_3F_2(\alpha_1, \alpha_2, \alpha_3; \beta_1, \beta_2; x)$ is a generalized hypergeometric function,³⁰ $\Gamma(x)$ is the Gamma function,^{25,30} $n_{\min} = \min(n', n'')$, and $n_{\max} = \max(n', n'')$. An equivalent representation of the integral Eq. (25) in the Coulomb matrix elements $\Delta_{n'n''}$ may be found in Ref. 8. Since for negative integers α_i ($i=1, 2$, or 3) the function ${}_3F_2(\alpha_1, \alpha_2, \alpha_3; \beta_1, \beta_2; x)$ is reduced to the polynomial of degree $-\alpha_i$, Eqs. (25) and (26) make our calculation scheme competitive with other approaches.^{6-8,10} Also, because of that, the procedure described here may be extended to the investigation of the excitons in quantum dots²⁷ or to calculations of the properties of quantum rings.³¹

The material parameters that we have used in our model calculation are given by

$$\begin{aligned}
\hbar\omega_0 = & 5 \text{ meV}, \quad m_e^* = 0.067m_e, \\
\epsilon = & 12.4, \quad g^* = -0.44,
\end{aligned}$$

where $\hbar\omega_0$ is the strength of the parabolic confinement. Hereafter, in order to distinguish the quantum numbers of the center of mass and relative motion, we shall use the subscripts a and b such that n_a and l_a indicate the quantum numbers for the former and n_b and l_b those for the latter.

The energy spectrum of the system considered is well known^{3,5-8,10} and therefore only the family of levels with $n_a=0$, $l_a=0$, $n_b=0$ and 1, and several l_b is presented in Fig. 1 (not including spin splittings) for completeness of the work without a detailed discussion associated with it. Here we simply point out that our numerical diagonalization scheme is very efficient and essentially exact in the sense that the accuracy can be improved as desired by taking more terms in Eq. (21). For instance, for the ground state at a

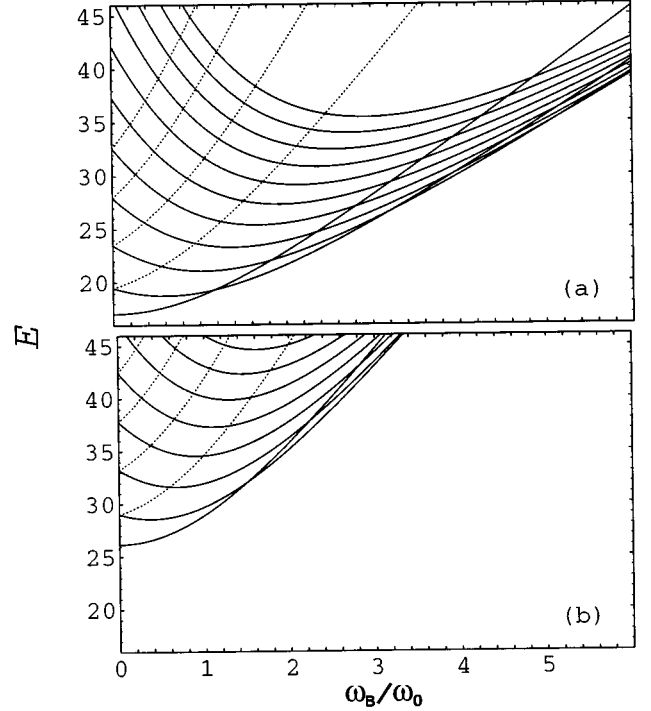


FIG. 1. Two-particle energies E associated with the spatial motion for fixed $n_a=0$ and $l_a=0$ in units of meV as a function of the ratio ω_B/ω_0 : (a) $n_b=0$ and (b) $n_b=1$. The solid curves are for $l_b=0, -1, -2, \dots$ and the dotted curves are for $l_b=1, 2, \dots$, labeled from below at the origin of the horizontal axis.

chosen $\omega_B/\omega_0=1$, the use of ten basis functions allowed the precision to be within the relative convergence of 2.4×10^{-4} . This accuracy was improved by almost an order of magnitude when 20 basis functions were taken.

In the following we shall focus our discussion on the resulting persistent currents of the system. Numerical accuracy similar to that for the energy eigenvalues was monitored for the persistent currents throughout the calculation. Let us first analyze the results at zero temperature, neglecting the spin effects. In this case, the net current I is simply given by Eq. (19) with the values of $J^{\text{c.m.}}$ and J^{rel} obtained at the ground state. The ground state is specified by the quantum numbers $n_a=0$, $l_a=0$, $n_b=0$, and a particular $l_b \leq 0$ depending on the magnitude of magnetic fields, as can be seen in Fig. 1. The orbital with $l_b=0$ remains as a ground state for the magnetic fields from zero up to some value. As the ratio ω_B/ω_0 increases the Coulomb interaction gives rise to a sequence of transitions in quantum numbers l_b .⁵ Before the first transition takes places, i.e., when the ground state is characterized by $l_b=0$, Eq. (24) dictates that the contribution from the relative motion is equal to that of an independent electron [see Eq. (6)]. Thus the net persistent current is exactly equal to that for noninteracting electrons and decreases linearly with magnetic fields. The result is illustrated in Fig. 2, where the current I is depicted as a function of the ratio ω_B/ω_0 : the solid curve is for interacting electrons and the dashed line is for independent electrons. This interesting aspect of the independence of the persistent current of the electron-electron interaction was recently predicted for the quantum ring.^{19-21,31} However, for the quantum dot it has

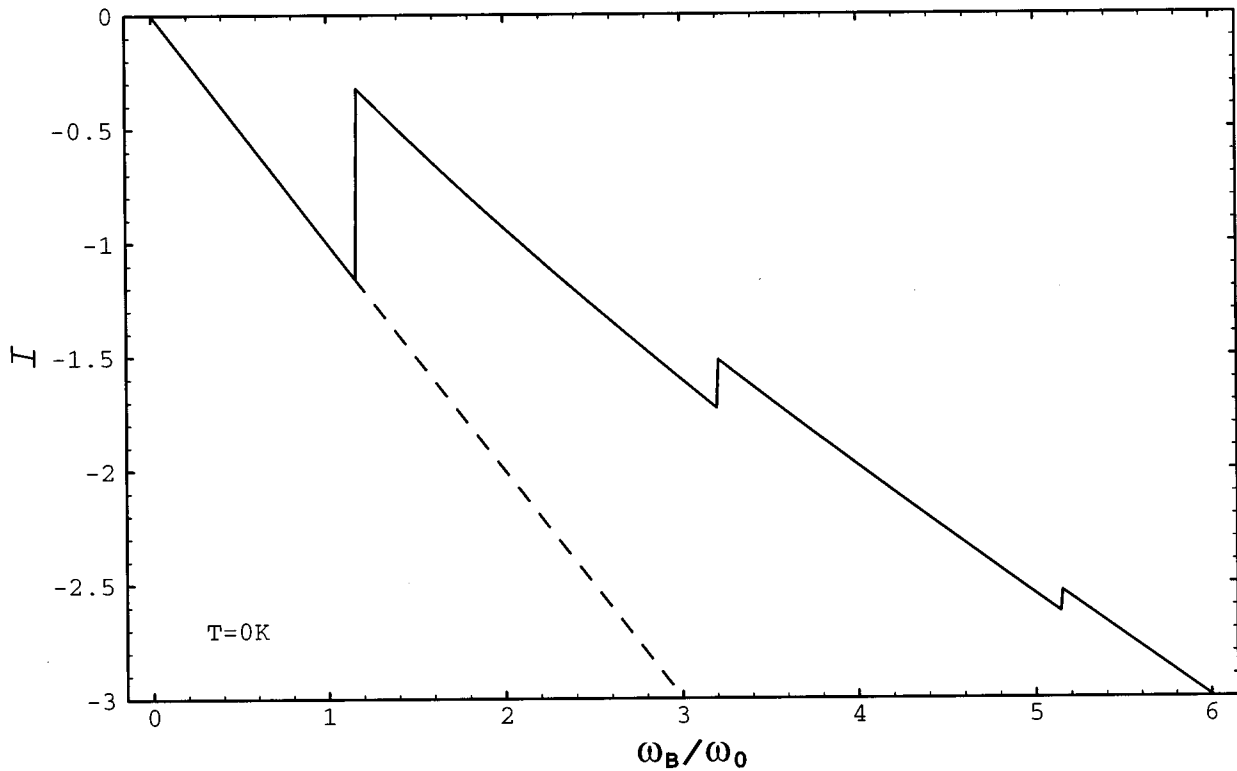


FIG. 2. Current I at zero temperature as a function of the ratio ω_B/ω_0 . The dashed curve is for independent electrons and the solid curve is for interacting electrons. Currents are in units of $e\omega_0/2\pi$.

local character in magnetic fields and is valid only for small fields. After the first transition of the ground state, the current will be determined by the state with $l_b = -1$. Therefore, at the point of the level crossing there appears a sudden change in the amplitude of the current, which is clearly reflected in Fig. 2. We note that the Coulomb interaction reduces the magnitude of the current and after the change the current shows a generally decreasing tendency with B . The next jumps are due to the similar transitions caused by the level crossings from $l_b = -1$ to $l_b = -2$ for the second jump, from $l_b = -2$ to $l_b = -3$ for the third jump, and so on. However, the current jumps at these points are smaller compared to the first crossing. Also, the size of the jumps decreases as the magnetic field increases. We have seen numerically that at very high magnetic fields ($\omega_B \gg \omega_0$) the current associated with the relative motion becomes negligible. Accordingly, the total current of the interacting electrons is one-half the current from the noninteracting picture. In Fig. 2, this means that the slope of the solid line is two times larger than that of the dotted line in the high-magnetic-field regime. On the other hand, it was reported that the corresponding magnetization tends to the value of the noninteracting system in the same limit.^{4,5} It is also worthwhile to note here that the location of the level crossings in Fig. 1 and, consequently, the position of the current jumps in Fig. 2 may be tuned by changing the parameters of the dot. In particular, it is known that the magnetic-field value, where the first spin-singlet and -triplet transition occurs, increases with $\hbar\omega_0$ (see, for instance, Fig. 3 in Ref. 8). Therefore, for smaller quantum dots these current jumps will occur at stronger fields, within the spinless-particle picture.

Now let us turn our attention to the finite-temperature calculation. Here we shall include the electron spins explicitly in the formulation so that the spin statistics plays an important role in determining relevant transport properties. The only minor approximation we adopt here is to presume that the definite current carried by the spin state is negligible compared to those from the spatial degrees of freedom, Eq. (19). In order to investigate thermodynamic properties at a finite temperature for a system with a fixed number of particles, it is essential to calculate the partition function. In the present problem the partition function is given by

$$Z = \text{Tr} e^{-\beta H(1,2)},$$

where Tr means the trace over two-particle states. We choose $|n_a, l_a; n_b, l_b; S, S_z\rangle$ as the simultaneous eigenkets of $H(1,2)$ in carrying out the trace. Considering the independence of the center of mass and the relative degree of freedom and also taking into account the exchange effect, it can be shown that the partition function is factorized into

$$Z = Z^{\text{c.m.}} (Z_{l_{\text{even}}}^{\text{rel}} Z_{S=0}^{\text{spin}} + Z_{l_{\text{odd}}}^{\text{rel}} Z_{S=1}^{\text{spin}}), \quad (27)$$

where $Z^{\text{c.m.}}$ indicates the partition function for the center-of-mass degree of freedom and $Z_{l_{\text{even}}}^{\text{rel}}$ and $Z_{l_{\text{odd}}}^{\text{rel}}$ represent the relative partition function having the partial sum of even and odd angular momentum states, respectively. The partition functions associated with the spin-singlet and spin-triplet states are specified to be

$$Z_{S=0}^{\text{spin}} = 1, \quad Z_{S=1}^{\text{spin}} = 1 + 2 \cosh(\beta g^* \mu_B B). \quad (28)$$

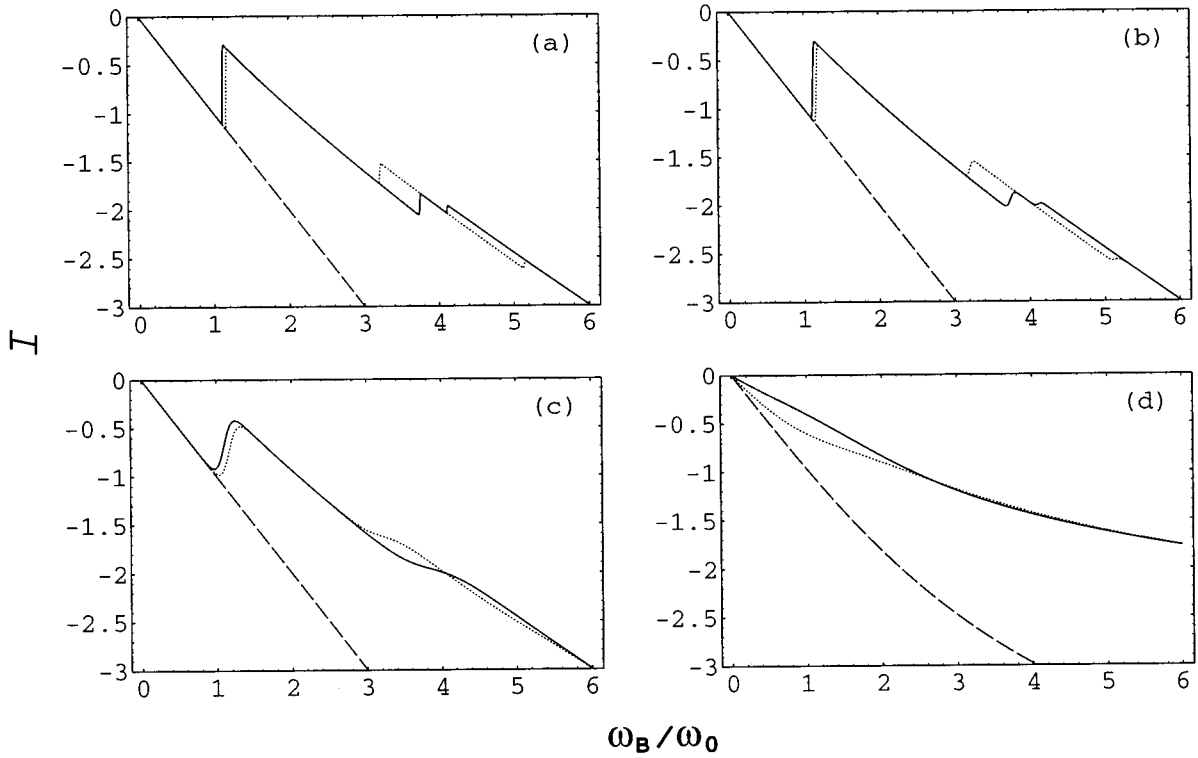


FIG. 3. Current I at finite temperature T as a function of the ratio ω_B/ω_0 : (a) $T=0.01$ K, (b) $T=0.1$ K, (c) $T=1$ K, and (d) $T=10$ K. The solid curves are with the exchange effect and the dotted curves are without the exchange effect, for interacting electrons; in addition, the dashed curves are inserted for the independent-electron model. The units of the currents are the same as in Fig. 2.

When the exchange effect is neglected, the full factorization approximation leads to

$$Z \approx Z^{\text{c.m.}} Z^{\text{rel}} Z^{\text{spin}} \approx 4Z^{\text{c.m.}} Z^{\text{rel}}, \quad (29)$$

where the second step is valid when the further limit of $|\beta g^* \mu_B B| \ll 1$ is taken. On the other hand, the limit of

$|\beta g^* \mu_B B| \gg 1$ leads to $Z^{\text{spin}} \rightarrow e^{-\beta g^* \mu_B B}$, which corresponds to the situation where the electron spins align along the magnetic field, i.e., the $S_z=1$ case. The persistent current I of principal interest now can be evaluated by taking the ensemble average of $J^{\text{c.m.}} + J^{\text{rel}}$, whose explicit expression is given by

$$I = \frac{1}{Z_{\text{c.m.}} \sum_{n_a} \sum_{l_a} J_{n_a, l_a}^{\text{c.m.}} e^{-\beta E_{n_a, l_a}^{\text{c.m.}}} + \frac{\sum_{n_b} \sum_{l_b}^{\text{even}} J_{n_b, l_b}^{\text{rel}} e^{-\beta E_{n_b, l_b}^{\text{rel}} Z_{S=0}^{\text{spin}}} + \sum_{n_b} \sum_{l_b}^{\text{odd}} J_{n_b, l_b}^{\text{rel}} e^{-\beta E_{n_b, l_b}^{\text{rel}} Z_{S=1}^{\text{spin}}}}{Z_{l_b, \text{even}}^{\text{rel}} Z_{S=0}^{\text{spin}} + Z_{l_b, \text{odd}}^{\text{rel}} Z_{S=1}^{\text{spin}}}}. \quad (30)$$

The results are manifested in Fig. 3 as solid curves as a function of the ratio ω_B/ω_0 , where currents are in units of $e\omega_0/2\pi$. The prominent features of sudden changes in the magnitude of the currents for low temperatures, at particular magnetic fields, again originate due to the alternating spin-singlet and -triplet transitions, as thoroughly discussed when explaining Fig. 2. Here we want to emphasize that this feature stems not from the spin effects but essentially from the crossings of the energy levels due to the interaction. It is observed that this structure diminishes as temperature increases and eventually disappears. A comparison with magnetization^{4,5} shows many similarities in its dependence on the temperature and the magnetic field. However, con-

trary to the magnetization that at high magnetic fields saturates to the value of the two independent electrons, the persistent currents of interacting electrons at high B that we obtained are different from those of the noninteracting picture (the dashed curves in Fig. 3). Our results show that due to the Coulomb interaction, the magnitudes of the persistent currents are reduced in general for all ranges of magnetic fields.

Another important aspect of Fig. 3 is the spin effect. The dotted curves are the outcome of the spinless-particle picture: neither the symmetry of the total wave function nor the spin splitting in energy was considered. The general tendency of smoothing out the jumps in currents with tempera-

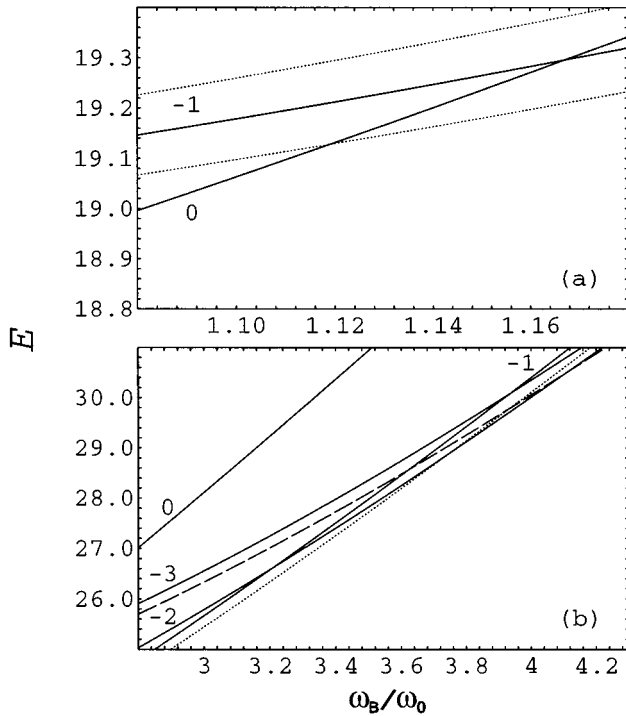


FIG. 4. Same as Fig. 1, but with $n_b=0$ for both cases: (a) solid curves are for $l_b=0$ and -1 without spin splittings and dotted curves are the spin splittings of the level $l_b=-1$; (b) solid curves are energy levels for $l_b=0, -1, -2,$ and -3 , as indicated, and the dotted and dashed curves are the lower-lying spin splittings of the levels $l_b=-1$ and -3 , respectively.

ture is similar to the exact calculations (solid curves). However, in detail there are differences in the locations where the sharp changes take places. For instance, the first jump of the exact outcome appears prior to the corresponding jump out of the spinless model. The precise location of these jumps in Fig. 3(a) can be identified through the energy spectrum, where the temperature is extremely low so that it is nearly equivalent to the zero-temperature results. [The dotted curve in Fig. 3(a) is identical to the solid line in Fig. 2.] For this purpose, in Fig. 4 we have plotted the relevant part of the energy spectra as the solid curve in Fig. 3(a). The dotted lines in Fig. 4(a) are the spin splittings for the state $l_b=-1$. Notice that there are no splittings for the level with $l_b=0$ since electrons are in the spin-singlet state in this case. It is clearly seen that the first jump of the solid curve in Fig. 3(a) occurs at the crossing point in the energy spectrum [Fig. 4(a)], where there exists the transition from $l_b=0$ to $l_b=-1$ (the lower-lying dotted curve). The crossing between two solid curves in Fig. 4(a) corresponds to the first jump in the dotted curve in Fig. 3(a) or the first jump in Fig. 2. This explains why the jump of the current appears first for the exact calculation compared to that of the spinless model: because of the spin splittings for the level $l_b=-1$ the ground state of the quantum dot considered undergoes the spin-singlet and -triplet transition at the weaker magnetic field compared to the threshold magnetic field for the spinless model. The differences in the other jumps in Fig. 3(a) can be similarly understood through Fig. 4(b), where the

dotted line and the dashed line are the lower-lying spin splitting of the levels $l_b=-1$ and $l_b=-3$, respectively. The higher-lying spin splittings have not been drawn since they do not participate in determining the ground state.

At finite temperatures, the thermal average occupancy of all energy levels is not zero and thus they will contribute to the transport properties of the system [see Eq. (30)]. Our results clearly manifest the importance of a proper treatment of the spin effect in investigating the thermodynamic properties of quantum dots. In the high-temperature limit, two results become identical, as indicated in Fig. 3(d).

IV. CONCLUSION

The persistent currents of two interacting electrons in a quantum dot have been calculated. It was found that at very low temperatures there was a range of weak magnetic fields where the current was not affected by the Coulomb interaction. However, the effect of the interaction is crucial for the higher magnetic fields, where the deviation from the noninteracting picture occurs as sudden drops of the magnitude of the current. The threshold value of the applied field at which the deviation occurs is seen to be influenced by the steepness of the confining potential of the quantum dots. The steeper the potential, the bigger the value of the fields. The pronounced abrupt change of the current at low temperatures is attributed to the alternative transition between the spin-singlet and -triplet states in the energy spectrum, essentially due to the interaction. Moreover, we manifested that a proper treatment of the spin effects, including the antisymmetry of the total wave function and the anomalous spin splittings in the energy, was important in determining the actual values of the magnetic fields, at which the quantum behaviors take places, for a given steepness of the confinement potential. Our results clearly showed the discrepancies between the exact calculation and the frequently used spinless-particle model: the latter is valid only in the high-temperature limit. Also, contrary to the magnetization, the current does not tend to the noninteracting value at strong magnetic fields. At finite temperature the aforementioned structure of the current is smoothed out and the current of the interacting system is always smaller than that of the outcome of the ideal case.

Throughout our calculations we assumed the parabolic confinement of the quantum dot. Recently, the energy spectra of the two-electron quantum disks with a hard-wall confinement have been calculated.¹⁴ This model is suitable for the $\text{In}_x\text{Ga}_{1-x}\text{As}/\text{GaAs}$ quantum dots. The results show that the ground state also exhibits the transition from the singlet to the triplet states. Accordingly, the results strongly suggest that the current jumps observed in our calculation will take place in these quantum dots too.

ACKNOWLEDGMENT

This work has been supported by the Ministry of Education of Korea through the Institute of Basic Sciences at Chonnam National University (Grant No. BSRI-96-2431).

- ¹P. A. Maksym and T. Chakraborty, Phys. Rev. Lett. **65**, 108 (1990).
- ²F. Geerinx, F. M. Peeters, and J. T. Devreese, J. Appl. Phys. **68**, 3435 (1990).
- ³U. Merkt, J. Huser, and M. Wagner, Phys. Rev. B **43**, 7320 (1991).
- ⁴P. A. Maksym and T. Chakraborty, Phys. Rev. B **45**, 1947 (1992).
- ⁵M. Wagner, U. Merkt, and A. V. Chaplik, Phys. Rev. B **45**, 1951 (1992).
- ⁶J.-J. S. De Groot, J. E. M. Hornos, and A. V. Chaplik, Phys. Rev. B **46**, 12 773 (1992).
- ⁷D. Pfannkuche, V. Gudmundsson, and P. A. Maksym, Phys. Rev. B **47**, 2244 (1993).
- ⁸D. Pfannkuche, R. R. Gerhardts, P. A. Maksym, and V. Gudmundsson, Physica B **189**, 6 (1993).
- ⁹Y. Avishai and M. Kohmoto, Phys. Rev. Lett. **71**, 279 (1993); Physica A **200**, 504 (1993).
- ¹⁰M. El-Said, Semicond. Sci. Technol. **10**, 1310 (1995); Solid State Commun. **97**, 971 (1996).
- ¹¹J. H. Oh, K. J. Chang, G. Ihm, and S. J. Lee, J. Korean Phys. Soc. **28**, S132 (1995).
- ¹²S. Oh and J. Y. Ryu, J. Korean Phys. Soc. **29**, 334 (1996).
- ¹³C. S. Kim and O. Olendski, Phys. Rev. B **53**, 12 917 (1996).
- ¹⁴F. M. Peeters and V. A. Schweigert, Phys. Rev. B **53**, 1468 (1996).
- ¹⁵R. C. Ashoori, H. L. Stormer, J. S. Weiner, L. N. Pfeiffer, K. W. Baldwin, and K. W. West, Phys. Rev. Lett. **71**, 613 (1993).
- ¹⁶A. Kumar, S. E. Laux, and F. Stern, Phys. Rev. B **42**, 5166 (1990).
- ¹⁷L. P. Lévy, G. Dolan, J. Dunsmuir, and H. Bouchiat, Phys. Rev. Lett. **64**, 2074 (1990).
- ¹⁸V. Chandrasekhar, R. A. Webb, M. J. Brady, M. B. Ketchen, W. J. Gallagher, and A. Kleinsasser, Phys. Rev. Lett. **67**, 3578 (1991).
- ¹⁹A. Müller-Groeling, H. A. Weidenmüller, and C. H. Lewenkopf, Europhys. Lett. **22**, 193 (1993); Phys. Rev. B **49**, 4752 (1994).
- ²⁰Y. Avishai and G. Braverman, Phys. Rev. B **52**, 12 135 (1995).
- ²¹L. Wendler, V. M. Fomin, and A. V. Chaplik, Solid State Commun. **96**, 809 (1995).
- ²²V. Fock, Z. Phys. **47**, 446 (1928).
- ²³C. G. Darwin, Proc. Cambridge Philos. Soc. **27**, 86 (1930).
- ²⁴R. B. Dingle, Proc. R. Soc. London Ser. A **211**, 500 (1952).
- ²⁵*Handbook of Mathematical Functions*, edited by M. Abramowitz and I. A. Stegun (Dover, New York, 1965).
- ²⁶L. D. Landau and E. M. Lifshitz, *Quantum Mechanics (Non-Relativistic Theory)* (Pergamon, New York, 1977), Sec. 115.
- ²⁷W. Que, Phys. Rev. B **45**, 11 036 (1992).
- ²⁸A. Matulis and F. M. Peeters, J. Phys.: Condens. Matter **6**, 7751 (1994).
- ²⁹A. P. Prudnikov, Yu. A. Brychkov, and O. I. Marichev, *Integrals and Series* (Gordon and Breach, New York, 1986), Vol. 2.
- ³⁰I. S. Gradshteyn and I. M. Ryzhik, in *Table of Integrals, Series and Products*, edited by A. Jeffrey (Academic, New York, 1980).
- ³¹P. Pietiläinen and T. Chakraborty, Solid State Commun. **87**, 809 (1993); T. Chakraborty and P. Pietiläinen, Phys. Rev. B **50**, 8460 (1994).